

QCD Evolution of Superfast Quarks

Adam J. Freese and Misak M. Sargsian

Department of Physics, Florida International University, Miami, FL 33199 USA

(Dated: November 20, 2015)

The recent high-precision measurements of nuclear deep inelastic scattering at high x and moderate $6 < Q^2 < 9 \text{ GeV}^2$ give a rare opportunity to reach the quark distributions in the *superfast* region, in which the momentum fraction of the nucleon carried by its constituent quark is larger than the total fraction of the nucleon at rest, $x > 1$. We derive the leading-order QCD evolution equation for such quarks with the goal of relating the moderate- Q^2 data to the two earlier measurements of superfast quark distributions at large $60 < Q^2 < 200 \text{ GeV}^2$ region. Since the high Q^2 measurements gave strongly contradictory estimates of the nuclear effects that generate superfast quarks, relating them to the high-precision, moderate- Q^2 data through QCD evolution allows us to clarify this longstanding issue. Our calculations indicate that the moderate- Q^2 data are in better agreement with the high- Q^2 data which require substantial high-momentum nuclear effects in the generation of superfast quarks.

Introduction: Quarks in nuclei possessing momentum fractions $x = \frac{AQ^2}{2M_A q_0} > 1$ (referred to as superfast quarks) represent one of the most elusive degrees of freedom in nuclei. Here M_A is the mass of the nucleus A , and $-Q^2$ and q_0 are the invariant momentum and energy transferred to the nucleus. Since no such quark can be generated by QCD dynamics confined to a single nucleon without inter-nucleon interactions, the probing of superfast quarks will require direct interplay between QCD and nuclear dynamics. One of the earlier theoretical studies of superfast quarks[1] showed that the nuclear dynamics responsible for the generation of such quarks is significantly short-range, thus opening a new window into the high-density realm of the nuclear force. Such dynamics include multi-nucleon short range correlations[1–3], explicit quark degrees of freedom such as 6-quark clusters[4], or single-quark momentum exchanges between strongly correlated nucleons[5].

One way of probing superfast quarks experimentally is the extraction of the nuclear structure function $F_{2A}(x, Q^2)$ in deep inelastic scattering (DIS) from nuclei at $x > 1$ [1, 3]. Such studies are part of the physics program of the 12 GeV energy upgrade of Jefferson Lab[6]. Superfast quarks can also be probed in more unconventional processes such as semi-inclusive nuclear DIS processes with tagged spectator nucleons[7, 8], DIS production in the forward direction with $x_F > 1$ or large transverse momentum dijet production in $p + A \rightarrow \text{dijet} + X$ reactions at LHC kinematics[2]. All such processes will probe QCD dynamics in the extreme nuclear conditions with the potential of opening up uncharted territory for nuclear QCD.

Experimental Evidence for Superfast Quarks: The first attempt to probe superfast quarks was made by the BCDMS collaboration[9] in measuring the nuclear structure function F_{2A} in deep-inelastic scattering of 200 GeV muons from a ^{12}C target. The experiment covered the region of $52 \leq Q^2 \leq 200 \text{ GeV}^2$ and $x \leq 1.3$, for the first time extracting the F_{2A} structure functions for $\langle Q^2 \rangle$ values of 61, 85 and 150 GeV^2 and $x = 0.85, 0.95, 1.05, 1.15$

and 1.30. For these regions the *per nucleon* F_{2A} has been fitted in the form:

$$F_{2A}(x, Q^2) = F_{2A}(x_0 = 0.75, Q^2)e^{-s(x-0.75)}, \quad (1)$$

obtaining $s = 16.5 \pm 0.6$ for the slope factor. Such an exponent required a larger strength in the high momentum distribution of the nucleons in nuclei than the simple mean field Fermi momentum distribution can provide. However the amount of short-range correlations needed to agree with the data was very marginal.

The second experiment was done by the CCFR collaboration[11] using the neutrino and antineutrino beams in which the *per nucleon* F_{2A} structure function for ^{56}Fe was measured in the charged current sector for $\langle Q^2 \rangle = 125 \text{ GeV}^2$ and $0.6 \leq x \leq 1.2$. The experiment did not measure the absolute magnitudes of F_{2A} , but obtained the slope of the x distribution in the form of Eq. (1), with the exponent being evaluated as $s = 8.3 \pm 0.7 \pm 0.7$. This result was in clear contradiction with the BCDMS result, requiring a much larger high-momentum component in the wave function of the ^{56}Fe nucleus. The required high-momentum component was somewhat larger than the one deduced from the quasi-elastic electroproduction in the $x > 1$ region[10, 12–16].

Recently, the structure functions for a set of nuclei (^2H , ^3He , ^4He , ^9Be , ^{12}C , ^{63}Cu , and ^{197}Au) have been measured at JLab[17] for a wide range of x (including $x > 1$) and Q^2 ($2\text{--}9 \text{ GeV}^2$). The structure functions F_{2A} extracted for the highest Q^2 ($6\text{--}9 \text{ GeV}^2$) data for the ^{12}C target in these measurements were used to check their relation to the BCDMS and CCFR structure functions. For this, in Ref. [17] the extracted *per nucleon* $F_{2A}(x, Q^2)$ was corrected for target mass (TM) effects using the relation[18]:

$$F_{2A}(x, Q^2) = \frac{x^2}{\xi^2 r^3} F_{2A}^{(0)}(\xi, Q^2) + \frac{6M^2 x^3}{Q^2 r^4} h_2(\xi, Q^2) + \frac{12M^4 x^4}{Q^4 r^5} g_2(\xi, Q^2), \quad (2)$$

where $h_2(\xi, Q^2) = \int_{\xi}^A u^{-2} F_{2A}^{(0)}(u, Q^2) du$ and $g_2(\xi, Q^2) =$

$\int_{\xi}^A v^{-2}(v - \xi)F_{2A}^{(0)}(v, Q^2)dv$, with Nachtmann variable $\xi = 2x/(1+r)$ and $r = \sqrt{1+Q^2/\nu^2}$. Here, $F_{2A}^{(0)}(\xi, Q^2)$ is the corrected structure function for which the Q^2 dependence should come from the evolution equation.

To relate the extracted $F_{2A}^{(0)}(\xi, Q^2)$ at large ξ to the BCDMS and CCFR results, in Ref. [17] the Q^2 dependence was fitted to the world data, including JLab's higher- Q^2 data, at several values of ξ . Then, using this fit, the extracted $F_{2A}^{(0)}(\xi, Q_0^2)$ at $Q_0^2 = 7 \text{ GeV}^2$ was extrapolated to the BCDMS and CCFR kinematics at large ξ . This extrapolation[17] resulted in the slope factor of $s = 15 \pm 0.5$ indicating that the JLab data are more consistent with the BCDMS results, with the latter showing only marginal strength of high momentum component of nuclear wave function[9](see above discussion).

However, to have the final answer on the relation of the JLab's structure functions to the higher Q^2 BCDMS and CCFR data one needs a full account of QCD evolution. To do so, we derive in the following section the QCD evolution equation for superfast quarks and apply it to $F_{2A}^{(0)}(\xi, Q_0^2)$, thus performing the evolution to BCDMS and CCFR kinematics.

Evolution Equation: We start with the leading order evolution equation for quarks in nuclei:

$$\begin{aligned} \frac{dq_{i,A}(x, Q^2)}{d \log Q^2} &= \frac{\alpha_s}{2\pi} \int_x^A \frac{dy}{y} \left(q_{i,A}(y, Q^2) P_{qq} \left(\frac{x}{y} \right) \right. \\ &\quad \left. + g_A(y, Q^2) P_{qg} \left(\frac{x}{y} \right) \right) \end{aligned} \quad (3)$$

with the goal of calculating the evolution for the *per nucleon* structure function F_{2A} defined as:

$$F_{2A}(x, Q^2) = \frac{1}{A} \sum_i e_i^2 x q_{i,A}(x, Q^2), \quad (4)$$

where one sums over the flavors of active quarks and antiquarks. Note that in Eq. (3) the upper limit of the integration is A , and thus the integrand in the range of $y > 1$ accounts for the contribution of the superfast quarks to the evolution of the partonic distribution $q_{i,A}$ probed at a given (x, Q^2) .

Above, the $q_{i,A}$ functions are the i -flavor quark and antiquark distributions in nuclei, while g_A represents the nuclear gluon distribution. The splitting functions are:

$$\begin{aligned} P_{qq}(x) &= C_2 \left[(1+x^2) \left(\frac{1}{1-x} \right)_+ + \frac{3}{2} \delta(1-x) \right] \\ P_{qg}(x) &= T [(1-x)^2 + x^2], \end{aligned} \quad (5)$$

with $C_2 = \frac{4}{3}$ and $T = \frac{1}{2}$. Here the $+$ denominator is the Altarelli-Parisi function, defined as[19]:

$$\int_0^1 dz \frac{f(z)}{(1-z)_+} = \int_0^1 \frac{f(z) - f(0)}{1-z}. \quad (6)$$

We proceed by changing the integration variable in Eq. (3) to $z = \frac{x}{y}$ which yields:

$$\begin{aligned} \frac{dq_{i,A}(x, Q^2)}{d \log Q^2} &= \frac{\alpha_s}{2\pi} \int_{x/A}^1 \frac{dz}{z} \left(q_{i,A} \left(\frac{x}{z}, Q^2 \right) P_{qq}(z) \right. \\ &\quad \left. + g_A \left(\frac{x}{z}, Q^2 \right) P_{qg}(z) \right). \end{aligned} \quad (7)$$

Substituting the splitting functions of Eq. (5) into the above equation results in:

$$\begin{aligned} \frac{dq_{i,A}(x, Q^2)}{d \log Q^2} &= \frac{\alpha_s}{2\pi} \left\{ 2q_{i,A}(x, Q^2) + \frac{4}{3} \int_0^1 dz \frac{f(z)}{(1-x)_+} \right. \\ &\quad \left. + \int_{x/A}^1 dz \frac{(1-z)^2 + z^2}{2z} g_A \left(\frac{x}{z}, Q^2 \right) \right\}, \end{aligned} \quad (8)$$

where

$$f(z) = \frac{1+z^2}{z} q_{i,A} \left(\frac{x}{z}, Q^2 \right) \theta \left(z - \frac{x}{A} \right). \quad (9)$$

Applying the rule of Eq. (6) into the second integral of Eq. (8), one obtains the final expression for the evolution equation of the quarks in the nucleus in the form:

$$\begin{aligned} \frac{dq_{i,A}(x, Q^2)}{d \log Q^2} &= \frac{\alpha_s}{2\pi} \left\{ 2 \left(1 + \frac{4}{3} \log \left(1 - \frac{x}{A} \right) \right) q_{i,A}(x, Q^2) \right. \\ &\quad + \frac{4}{3} \int_{x/A}^1 \frac{dz}{1-z} \left(\frac{1+z^2}{z} q_{i,A} \left(\frac{x}{z}, Q^2 \right) - 2q_{i,A}(x, Q^2) \right) \\ &\quad \left. + \int_{x/A}^1 dz \frac{(1-z)^2 + z^2}{2z} g_A \left(\frac{x}{z}, Q^2 \right) \right\}. \end{aligned} \quad (10)$$

This equation can be used to obtain the evolution equation for the structure function F_{2A} defined according to Eq. (4). Multiplying both sides above by $e_i^2 x$ and summing by contribution of all quarks and antiquarks one obtains the evolution equation for the nuclear structure function F_{2A} in the form:

$$\begin{aligned} \frac{dF_{2A}(x, Q^2)}{d \log Q^2} &= \frac{\alpha_s}{2\pi} \left\{ 2 \left(1 + \frac{4}{3} \log \left(1 - \frac{x}{A} \right) \right) F_{2,A}(x, Q^2) \right. \\ &\quad + \frac{4}{3} \int_{x/A}^1 \frac{dz}{1-z} \left(\frac{1+z^2}{z} F_{2A} \left(\frac{x}{z}, Q^2 \right) - 2F_{2A}(x, Q^2) \right) \\ &\quad \left. + \frac{f_Q}{2} \int_{x/A}^1 dz [(1-z)^2 + z^2] \frac{x}{z} G_A \left(\frac{x}{z}, Q^2 \right) \right\}. \end{aligned} \quad (11)$$

where $f_Q = \sum_i (e_i^2 + \bar{e}_i^2)$ and $G_A(x, Q^2) = x g_A(x, Q^2)/A$. One interesting property of the above equation which has

a nuclear origin is the factor $\log(1 - \frac{x}{A})$ which introduces a non-trivial A dependence into the evolution equation. The effect of this term can be observed for light nuclei at large x kinematics.

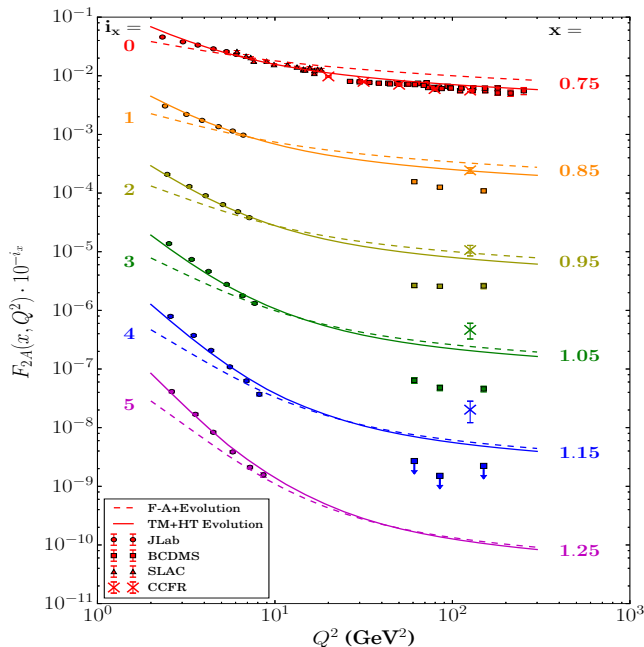


FIG. 1: (Color online.) Comparison of evolution equation results for the *per nucleon* F_{2A} of ^{12}C to experimental measurements. The structure function is multiplied by 10^{-i_x} in order to separate the curves; the values of i_x for each x value are given in the plot.

Evolution of F_{2A} from moderate to high Q^2 : At large $x > 0.1$, we can safely neglect the gluonic distribution G_A in Eq. (11), after which the evolution of the structure function F_{2A} at given (x, Q^2) will be defined by the same structure function at $x' \geq x$ and some initial Q_0^2 . Such a situation allows us to relate the F_{2A} structure functions at high- Q^2 (BCDMS and CCFR) kinematics to the same structure function at moderate- Q^2 (JLab) kinematics using Eq. (11), without requiring the knowledge of the nuclear gluonic distribution G_A .

To do so, first, we use as an input to Eq. (11) the same parametrization of $F_{2A}^{(0)}(\xi, Q_0^2)$ at $Q_0^2 = 7 \text{ GeV}^2$ [20] for the ^{12}C nucleus that was used in high- ξ and high- Q^2 extrapolation of Ref. [17] (referred to hereafter as the F-A parameterization). With this input, Eq. (11) is solved numerically, covering the Q^2 range of 2-300 GeV^2 . The TM-uncorrected F_{2A} is then obtained from $F_{2A}^{(0)}$ by reintroducing target mass effects according to Eq. (2).

The result of the calculations is given by the dashed curves in Fig. 1, along with experimental data and SLAC “pseudodata.” The JLab[17] and BCDMS[9, 23] data are measurements of the structure function per nucleon, whereas the SLAC pseudodata are obtained according to Ref. [17] by multiplying deuteron F_2 measurements[21]

by the EMC ratio measured in Ref. [22]. The CCFR data at $x > 0.75$ were given without an absolute normalization[11], so in Fig. 1 the $x = 0.75$ point was normalized to the previous CCFR measurement at $x \leq 0.75$, for which the absolute values have been measured[24].

As the figure shows, the F-A parameterization extended to the high- Q^2 domain of the CCFR and BCDMS experiments ($Q^2 \sim 125 \text{ GeV}^2$) through QCD evolution does not prefer the BCDMS data as the Q^2 extrapolation of Ref. [17] had indicated. In fact, QCD evolution of JLab data shows better agreement with the CCFR data at $x \leq 1.05$, and results in a slope factor $s = 13 \pm 0.4$ for the range of $0.75 \leq x < 1.25$.

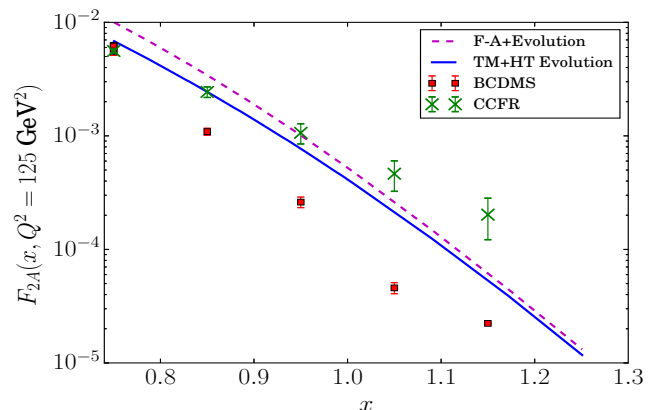


FIG. 2: The x dependence of F_{2A} at $Q^2 = 125 \text{ GeV}^2$

Target Mass and Higher Twist Corrections: Even though QCD evolution of the F-A parameterization predicts softer x dependence for $F_{2A}(x)$ at $Q^2 = 125 \text{ GeV}^2$ ($s = 13 \pm 0.4$, compared to $s = 15 \pm 0.5$ in Ref. [17]), it overestimates the F_{2A} at $x = 0.75$ (see Fig. 2). We attribute this overestimation to the higher twist (HT) effects for which JLab data have not been corrected.

To check the validity of our conjecture, we analyzed the uncorrected JLab data for both TM and HT effects within a framework of Ref. [26]. In the analysis, we used the fact that the overall TM+HT correction is insensitive to the particular method of the TM correction, since the HT correction largely eliminates the differences between various TM approaches. Accordingly, we adopted for the TM correction the ξ -scaling prescription, which in the leading order approximation corresponds to the TM correction in the collinear approximation[27]. For the HT correction, we parameterized the JLab data in the form[26]

$$F_{2A}(\xi, Q^2) = F_{2A}^{\text{LT}}(\xi, Q^2) \left(1 + \frac{c_1 \xi^{c_2} (1 + c_3 \xi)}{Q^2} \right), \quad (12)$$

to extract the leading twist (LT) structure function $F_{2A}^{\text{LT}}(\xi, Q^2)$ (for details see Ref. [28]). The latter was used as an input to the QCD evolution equation (Eq. (11)) to calculate F_{2A} for the CCFR and BCDMS kinematics.

In Figs. 1 and 2, the solid curves represent the results of the above calculation. At $Q^2 \leq 9 \text{ GeV}^2$ they are the fits according to Eq. (12), while higher Q^2 range is obtained through the QCD evolution of the leading-twist structure function $F_{2A}^{\text{LT}}(\xi, Q^2)$. As the comparison shows, QCD evolution now describes reasonably well the $x = 0.75$ data at $Q^2 = 125 \text{ GeV}^2$. For the slope factor, one obtains $s = 12.3 \pm 0.4$, which is somewhat in the middle of the CCFR ($s \approx 8.3$) and BCDMS ($s \approx 16.5$) estimates, while the absolute magnitude of F_{2A} is closer to the CCFR data at $x \leq 1.05$.

NLO Corrections: To estimate the accuracy of leading order evolution equation presented in Figs. 1 and 2, we calculated also the next-to-leading order (NLO) corrections to the evolution of F_{2A} . In NLO the evolution equation cannot be presented as a single equation such as Eq. (11) where F_{2A} evolves by itself. Instead, in NLO we calculate the evolution of each quark distribution separately, and then construct F_{2A} according to Eq.(4).

Numerical computations of NLO evolution[28] are performed by constructing singlet and non-singlet quark mixtures[25], and approximating all quark and antiquark distributions except u and d as zero for the initial Q_0^2 . The NLO corrections decrease F_{2A} at $Q^2 = 125 \text{ GeV}^2$ by 9% and 13% for $x = 0.75$ and $x = 1.25$ respectively, which results in the increase of the slope factor s by

$\sim \log(0.91/0.87)/1.25 \approx 0.036$ which does not change the conclusion made within the LO approximation.

Summary: We derived the evolution equation for superfast quarks in nuclei in leading order approximation. For the F_{2A} structure function at high x , in an approximation in which the gluon distribution is neglected, QCD evolution is defined by the same F_{2A} measured at some initial value of Q_0^2 . Using this property and the parameterization of F_{2A} at moderate $Q^2 = 7 \text{ GeV}^2$, corrected for TM and HT effects, we calculated the F_{2A} for the range of $60 < Q^2 < 200 \text{ GeV}^2$ at which the previous measurements of superfast quark distributions have been made. Our calculation demonstrates that the JLab high-precision, moderate- Q^2 measurement of the ^{12}C structure function is in better agreement with the CCFR data at $Q^2 = 125 \text{ GeV}^2$ and $x \leq 1.05$ with the slope factor s indicating on the substantial contribution of the high-momentum nuclear component in the generation of superfast quarks.

Acknowledgement: We are thankful to Drs. John Arrington and Nadia Fomin for numerous discussions and providing results of their analysis and the fit of the Carbon structure function of their Jefferson Lab experiment. This work is supported by U.S. DOE grant under contract DE-FG02-01ER41172.

-
- [1] L. L. Frankfurt and M. I. Strikman, Phys. Rept. **160**, 235 (1988).
 - [2] A. J. Freese, M. M. Sargsian and M. I. Strikman, Eur. Phys. J. C **75**, no. 11, 534 (2015).
 - [3] M. Sargsian, J. Arrington, *et al.*, J.Phys. G**29**, R1 (2003).
 - [4] C. Carlson and K. Lassila, Phys. Rev. C **51**, 364 (1995).
 - [5] M. M. Sargsian, Nucl. Phys. A **782**, 199 (2007).
 - [6] J. Arrington, D. Day, N. Fomin and P. Solvignon, (spokespersons) *Inclusive Scattering from Nuclei at $x > 1$ in the quasielastic and deeply inelastic regimes* Jefferson Lab Proposal, PR12-06-105, 2006.
 - [7] W. Melnitchouk, M. Sargsian and M. I. Strikman, Z. Phys. A **359**, 99 (1997).
 - [8] W. Cosyn, M. Sargsian, Phys. Rev. C**84**, 014601 (2011).
 - [9] A. C. Benvenuti *et al.* [BCDMS Collaboration], Z. Phys. C **63**, 29 (1994).
 - [10] L. L. Frankfurt, M. I. Strikman, D. B. Day and M. M. Sargsian, Phys. Rev. C **48**, 2451 (1993).
 - [11] M. Vakili *et al.* [CCFR Collaboration], Phys. Rev. D **61**, 052003 (2000).
 - [12] K. S. Egiyan *et al.*, Phys. Rev. C **68**, 014313 (2003).
 - [13] K. S. Egiyan *et al.*, Phys. Rev. Lett. **96**, 082501 (2006).
 - [14] N. Fomin *et al.*, Phys. Rev. Lett. **108**, 092502 (2012).
 - [15] M. M. Sargsian, Phys. Rev. C **89**, no. 3, 034305 (2014).
 - [16] M. McGauley, M.M. Sargsian, arXiv:1102.3973 [nucl-th].
 - [17] N. Fomin *et al.*, Phys. Rev. Lett. **105**, 212502 (2010).
 - [18] I. Schienbein *et al.*, J. Phys. G **35**, 053101 (2008).
 - [19] G. Altarelli and G. Parisi, Nucl. Phys. B **126**, 298 (1977).
 - [20] J. Arrington and N Fomin *Private Communcation*
 - [21] L. W. Whitlow, E. M. Riordan, S. Dasu, S. Rock, and A. Bodek, Phys. Lett. **B282**, 475 (1992).
 - [22] J. Gomez *et al.*, Phys. Lett. **B282**, 475 (1992).
 - [23] A. C. Benvenuti *et al.* [BCDMS Collaboration], Phys. Lett. **B195**, 91 (1987).
 - [24] W. G. Seligman *et al.*, Phys. Rev. Lett. **79**, 1213 (1997).
 - [25] R. K. Ellis, W. J. Stirling and B. R. Webber, Camb. Monogr. Part. Phys. Nucl. Phys. Cosmol. **8**, 1 (1996).
 - [26] A. Accardi *et al.*, Phys. Rev. D **81**, 034016 (2010).
 - [27] M. Aivazis *et al.*, Phys. Rev. D **50**, 3085 (1994).
 - [28] A. Freese and M.M. Sargsian, *Supplementary material*.